Acta Mineralogica-Petrographica, Szeged 2006–2007, Vol. 47, pp. 17-24

ACTA Mineralogica Petrographica

MICRO-RAMAN SPECTROSCOPY OF REIDITE AS AN IMPACT-INDUCED HIGH PRESSURE POLYMORPH OF ZIRCON: EXPERIMENTAL INVESTIGATION AND ATTEMPT TO APPLICATION

ARNOLD GUCSIK

Max Planck Institute for Chemistry, Department of Geochemistry, Joh.-J.-Becherweg 27. Mainz, D-55128, Germany
e-mail: gucsik@mpch-mainz.mpg.de

ABSTRACT

Thorough understanding of the shock metamorphic signatures of zircon will provide a basis for the application of this mineral as a powerful tool for the study or recognition of old, deeply eroded, and metamorphically overprinted impact structures and formations. This study of the micro-Raman spectroscopic signatures of naturally shocked (Ries Crater, Germany) zircon crystals and experimentally (38, 40, 60, and 80 GPa) shock-metamorphosed single crystals of zircon contributes to the understanding of the formation of shock-induced microdeformations and phase transformation in zircon under very high, dynamic pressures. The purpose of this investigation is to further investigate the capability of the Raman spectroscopy to document shock deformation and to determine whether specific Raman effects in zircon/scheelite-structure (reidite) can be utilized to determine particular shock pressure stages.

Key words: zircon, high-pressure polymorph, reidite, shock metamorphism, Raman spectroscopy

INTRODUCTION

Zircon is a highly refractory and weathering-resistant mineral that has proven useful as a shock level indicator of shock metamorphism in the study of impact structures and formations that are old, deeply eroded, and metamorphically overprinted (e.g., Bohor et al. 1993, Kamo et al. 1996, Krogh et al. 1996, Reimold et al. 2002, Wittmann et al. 2006). Zircon has advantages compared to quartz or other shock-metamorphosed rock-forming minerals that have been widely used as impact indicators, but are far less refractory than zircon. Furthermore, U-Pb dating of zircon can provide constraints on the ages of impact events or deposition of impact formations (e.g., Deutsch and Schärer 1990, Kamo et al. 1996, and references therein). Table 1 shows the main physical and optical properties of zircon, baddaleyite, and reidite.

Shock metamorphic effects in zircon have been described from a number of impact environments, including confirmed impact structures (e.g., Kamo and Krogh 1995, Krogh et al. 1996, Kamo et al. 1996, Gibson et al. 1997, Glass and Liu 2001), the Cretaceous-Tertiary boundary (Bohor et al. 1993, Kamo and Krogh 1995), and the Upper Eocene impact ejecta layer (e.g., Glass and Liu 2001), as well as from tektites (Deloule et al.

Table 1. Basic physical and optical properties of zircon, baddeleyite and reidite.

Chemical Formula (name)	**$ZrSiO_4$** (zircon)	***ZrO_2*** (baddeleyeite)	***$ZrSiO_4$*** (reidite)
Z (formula units per unit cell)	4	4	4
Crystal System	*Tetragonal* Ditetragonal Dipyramidal (H-B Symbol: 4/m 2/m 2/m)	*Monoclinic-* Prismatic (H-B Symbol: 2/m)	*Tetragonal-* Dipyramidal (H-B Symbol: 4/m)
Space Group	$I\,4_1/amd$	$P\,2_1/c$	$I\,4_1/a$
Cell Dimensions (Á)	a=6.604 c=5.979	a=5.1477 b=5.203 c=5.3156	a=4.738 c=10.506
Axial Ratios	a:c=1:0.90536	a:b:c=0.9893:1:1.0216	a:c=1:2.21739
Density (g/cm^3)	4.6-4.7, average=4.65	5.5-6, average=5.75	5.2
Optical Data	Uniaxial (-) ε=1.92-1.96 ω=1.967-2.015 bire=0.047-0-055	Biaxial (-) Refractive index varies from 2.13 to 2.20 bire=0.07	Uniaxial (+) ε=1.655 ω=1.64 bire=0.015
Cleavage	[001] Indistinct	[001] Distinct	None
Fracture	Uneven-Flat surfaces (not cleavage) fractured ina n uneven pattern	Brittle-Conchoidal-Very brittle fracture producing small, conchoidal fragments	Brittle-Irregular-Very brittle fracture producing irregular fragments

Data from: http://euromin.w3sites.net/mineraux, and http://webmineral.com/AtoZ/IndexB.shtml

2001, Glass and Liu 2001). Shock-induced microdeformation in experimentally shock-deformed zircon crystals has also been reported (Deutsch and Schärer 1990, Leroux et al. 1999, Gucsik et al. 2002).

The phase transformation from the zircon crystal structure (ZrSiO4) to a scheelite (CaWO4)-structure phase as reidite was described in shock-metamorphosed zircon by Kusaba et al. (1985) to begin at about 30 GPa and to be complete at around 53 GPa. These observations were confirmed by Leroux et al. (1999) through their TEM investigations of experimentally shocked zircon. More recently, according to Scott et al. (2002), high-pressure X-ray data show that a small amount of residual zircon-structured material remained at 39.1 GPa on ZrSiO4-scheelite material. Glass et al. (2002) found the scheelite-type phase (reidite) in zircon samples from marine sediments from an upper Eocene impact ejecta layer sampled near New Jersey and Barbados. They named this mineral phase 'reidite' after Alan F. Reid, who first produced this high shock-pressure polymorph of zircon (Reid and Ringwood 1969).

This review study has been based on Gucsik et al. (2004) published In Dypvik, H., Burchell, M., Claeys, Ph. (eds.): Cratering in Marine Environments and on Ice, Springer-Verlag, Heidelberg, 281-322, emphasizing manly the micro-Raman spectroscopy and its application to study of high-pressure polymorphs associated to the impact terrestrial cratering record.

Samples and experimental procedures

Two natural zircon crystals of about 1 cm length and 0.5 and 0.7 cm width from Australia (sample A) and from Sri Lanka (sample B), respectively, were experimentally shock deformed at shock pressures between 38 and 80 GPa at room temperature. Shock recovery experiments were performed on such plates using the shock reverberation technique at the Ernst-Mach-Institute, Germany (e.g., Deutsch and Schärer 1990). For this study, polished thin sections, produced from the experimentally shocked plates of zircon crystals (A and B sample sets), were utilized. However, only the specimens from A sample were selected for further CL- and Raman spectroscopic investigations, because the sections are of better quality than those from sample B. Carbon-coated, polished thin sections had been produced from all samples. The samples were first examined under a petrographic microscope. Raman spectra were obtained with a Renishaw RM1000 confocal micro-Raman spectrometer (at University of Vienna, Austria) with a 20 mW, 632 nm He-Ne laser excitation system and a thermo-electrically cooled CCD detector. The power of the laser beam on the sample was approximately 3 mW. Spectra were obtained in the range

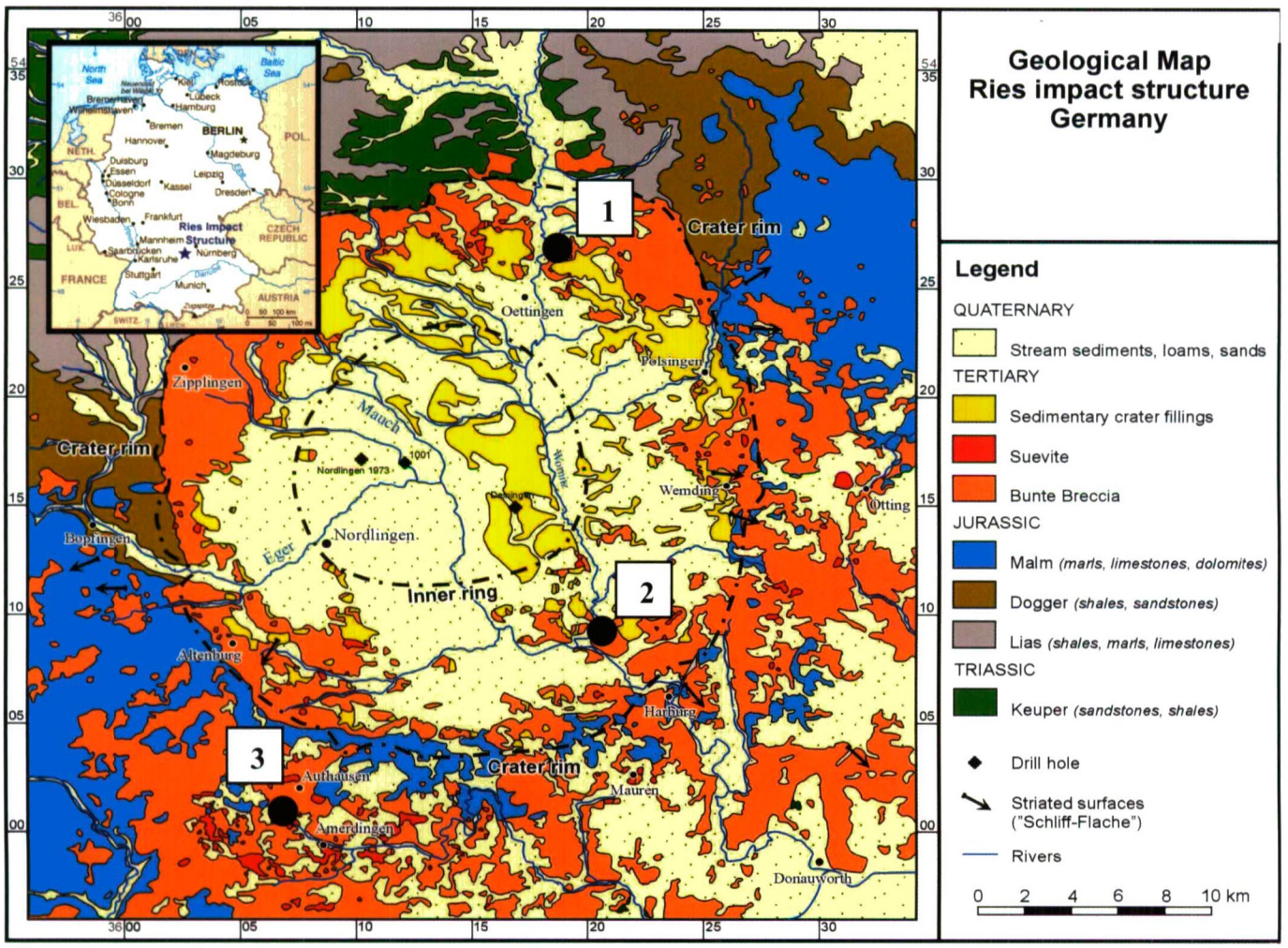

Fig. 1. Locality of the Ries basin in Germany and approximate extent of the Bunte Breccia and suevite breccia. Sample localities are indicated as ● 1=Aumühle, 2=Appertshofen, 3=Seelbronn (from Osinski et al. 2003).

100-1200 cm-1, with approximately thirty seconds total exposure time. The spectral resolution was 4 cm-1. Raman spectra were taken from 3 μm3 sample volume. Further details on the experimental procedure and samples can be found in Gucsik et al. (2004).

Regional geology of the Ries impact crater

The Ries (also called "Nördlinger Ries") is a complex impact structure, located in Southern Germany (centered at: N 48o53', E 10o37'), with a rim-to-rim diameter of about 26 km (e.g., Engelhardt 1990, Deutsch 1998). The well-preserved ejecta blanket (Geologische Karte des Rieses, Bayerisches Geologisches Landesamt, 1: 50 000, 1999) and intra-crater breccia lens offer excellent conditions for studies of terrestrial impact structures (e.g., Engelhardt 1990) (Fig. 1). According to the level of shock metamorphism, the ejecta from the Ries crater divided into two formations: (1) Low shock level (<10 GPa), represented by the Bunte Breccia (sediments from the upper 600 m of the target area), megablocks of sedimentary rocks (Upper Jurassic limestone blocks occurring in the Megablock zone), and megablocks and monomict breccias derived from the crystalline basement (from the surrounding area of the Inner Crater). (2) High shock level (>10 GPa), represented by polymict crystalline breccias (are common in the Megablock Zone), fall-out suevites, crater suevite, and tektites (moldavites) (Engelhardt 1990). A 15 Ma age was determined for the Ries impact by the 40Ar-39Ar method on impact glasses from suevitic impact breccias (Staudacher et al. 1982). The present structure formed as the result of the collapse of the transient impact crater by subsurface readjustment, which caused upward movement of the initial crater bottom and slumping of parts of the primary rim into the crater, producing a compensating ring depression (the so-called Megablock Zone) (Engelhardt 1990). The pre-impact stratigraphy of the target region includes a crystalline basement of pre-Variscan gneisses and amphibolites, and Variscan granite. These crystalline rocks were overlain by sedimentary rocks of Upper Jurassic (limestone), Middle Jurassic (sandstone, marlstone, limestone), Lower Jurassic (sandstone, marlstone, limestone), Upper Triassic (sandstone, siltstone, marlstone, claystone) and Lower Triassic (sandstone) age. The southern part of the target area was covered by ~25 m of unconsolidated Upper Miocene sands, marls and clays (Engelhardt 1990) (Fig. 2).

According to Stöffler (1974) and Engelhardt (1990), the stages of shock metamorphism in minerals from the impact formations of the Ries impact crater can be classified into six stages (known as 0, I, II, III, IV, and V) that are characterized by various elastic and plastic deformation phenomena as well as isotropization of minerals, the formation of high-pressure phases and the occurrence of mineral or bulk rock melting (Table 2).

Basics of Raman spectroscopy

According to Roberts and Beattie (1995), when a monochromatic beam of light illuminates a transparent medium (e.g., gas, liquid or solid), most of the light will traverse the

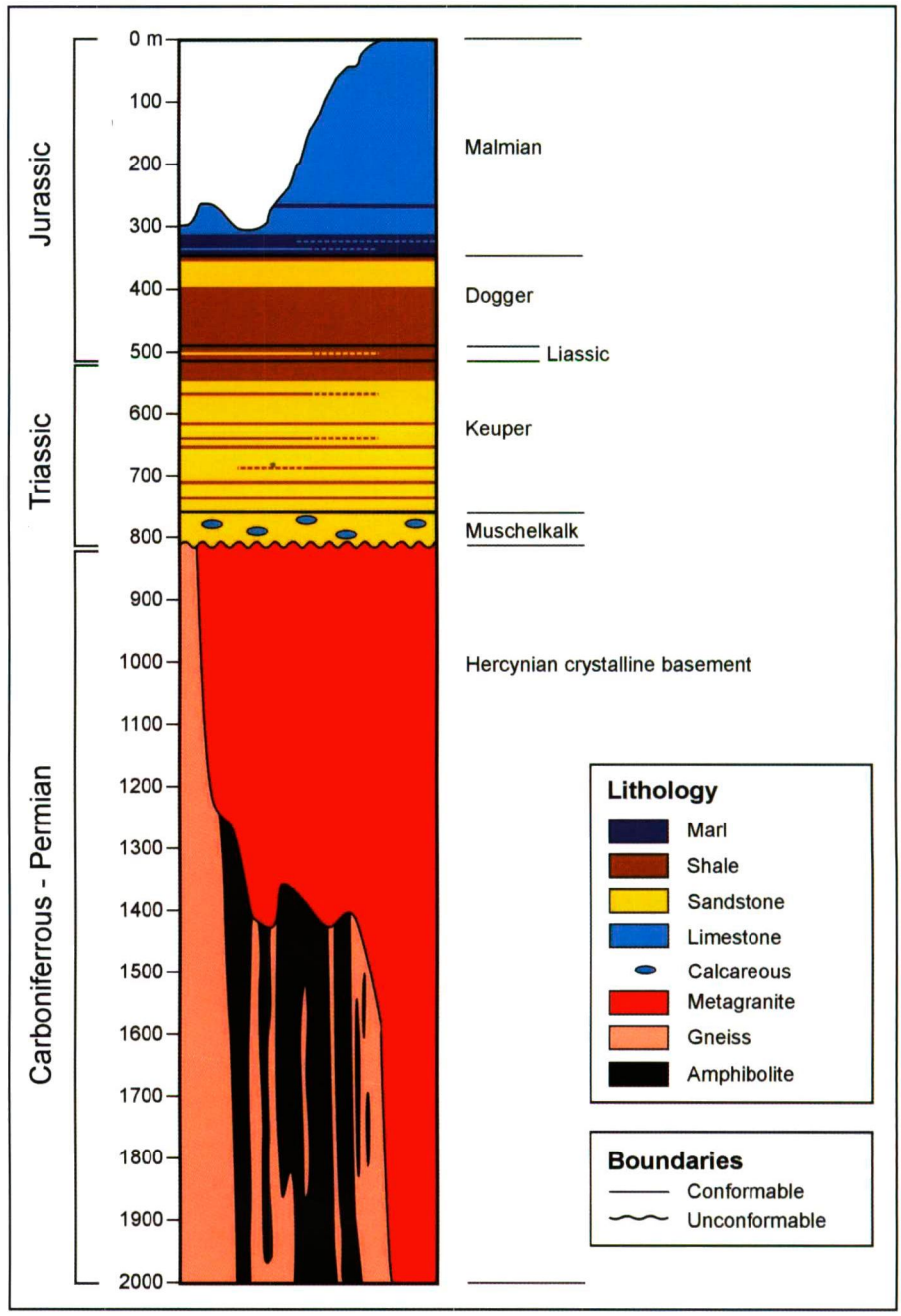

Fig. 2. The idealized stratigraphic sketch of the Ries carter exhibits the pre-and post impact stratigrapy (after Osinski et al. 2003).

sample without undergoing any changes. Approximately 10-3 of the incident intensity is scattered with the same frequency as that of the incident light source (elastic or Rayleigh scattering). Raman scattering ("Raman effect") occurs when, in addition to the Rayleigh scattering, about 10-6 of the incident intensity is scattered at new frequencies above and below the incident frequency. This effect was first documented by the Indian physicist Chandrasekhara Venkata Raman in 1928, who observed color changes in the scattered light of focused sunlight. The shifts in frequency from that of the incident radiation are independent of the exciting radiation and are characteristic of the species that gives rise to the scattering.

Raman transitions to lower frequency (i.e., red shifted bands) are referred to as Stokes lines, whereas transitions to higher frequency (i.e., blue shifted bands) are referred to as anti-Stokes lines. Stokes lines are normally much more intense than anti-Stokes lines, as the population of the ground state is usually very much greater than that of the excited state of the molecule. Not all molecular vibrations are Raman active. A Raman active vibration can be expected if the polarizability in a molecule is changed during the normal vibration (Roberts and Beattie 1995). The frequencies of vibrations depend upon the vibrating masses and the forces between them, including the anharmonic nature of interatomic and inter-and intramolecular interactions. If a phase transition occurs, the Raman selection rules, which ultimately depend on crystal and molecular symmetries, will also change (as well as forces) and new spectral features, characteristics for the new lattice, will appear (e.g., Williams and Knittle 1993, Nasdala et al. 1995). Thus, this method is not only of great help in elucidating crystal structures (e.g., McMillan and Hofmeister 1988), but can also be used as a method of qualitative analysis, e.g., in determining the presence of specific phases of small thin section areas without destroying them.

Table 2. Stages of shock metamorphism in the Ries impact structure, Germany (after Engelhardt, 1990).

Stage	Shock effects	Pressure (GPa)	Post-shock Temp. (°C)
0	Fragmentation; mosaicism; undulatory extinction; deformation bands in quartz; kinkbands in biotite; shatter cones	0-10	0-100
I	Planar elements in quartz; planar deformation lamellae in feldspar, amphibole and pyroxene; stishovite, coesite; kink bands in biotite	10-35	100-300
II	Diaplectic glasses of quartz and feldspar; deformation lamellae in amphibole and pyroxene; kinkbands in biotites	35-45	300-900
III	Selectively fused alakali-rich feldspar; diaplectic quartz glass; thermal decomposition of biotite and amphibole	45-50	900-1300
IV	Complete fusion of rocks (granitic composition); impact melts	60-80	1500-3000
V	Vaporization	>80	>3000

RAMAN SPECTROSCOPY OF EXPERIMENTALLY SHOCK-DEFORMED ZIRCON SAMPLES

The Raman spectra of the unshocked and experimentally shock-deformed zircon samples (38, 40, 60 and 80 GPa) show significant differences (Fig. 3). The Raman spectra of the unshocked samples (parallel) contain seven peaks at 202, 215, 225, 356, 439, 974, 1008 cm-1 (Fig. 3A) indicating the zircon-type structure (Williams and Knittle 1993, Kolesov 2001). Whereas all these peaks are characteristic for the zircon-type structure, the bands at 356 439, 974 and 1007 cm-1 appear most useful to distinguish this phase from the scheelite-type structure as reidite (Fig. 3A). It is important to note that the narrow line widths of the Raman bands of both unshocked samples indicate a highly crystalline structure without major zoning or defects.

The spectra of the 38 GPa samples (parallel) are dominated by a number of peaks at 204, 223, 238, 296, 325, 356, 404, 464, 556, 609, 846, and 883 cm-1. These peaks are characteristic for the reidite (Williams and Knittle 1993). This sample contains an additional peak at around 1000 cm-1 (Fig. 3B), which will be discussed below.

In the 40 GPa samples, typical reidite peaks occur at 204, 238, 296, 327, 356, 404, 464, 558, 610, 847, and 887, (Fig. 3C). In addition, relatively weak peaks appear at 223, 437 and 1005 cm-1 in the spectrum (Fig. 3C).

The Raman spectra of the 60 GPa samples (parallel) show peaks at 204, 238, 297, 327, 353, 406, 464, 558, 610, 847 and 887 cm-1 (Fig. 3D). The peak intensities of these peaks in both samples are approximately equal and all peaks are characteristic for the reidite. It is important to note that these peaks are totally different from the Gucsik et al. (2002), who observed an amorphous state without any vibration modes of Raman spectrum at 60 GPa.

The Raman spectra of the 80 GPa samples exhibit peaks that are typical for reidite at 205, 238, 297, 327, 353, 406 (relatively strong), 464, 558, 610, 847 and 887 cm-1 (Fig. 3E).

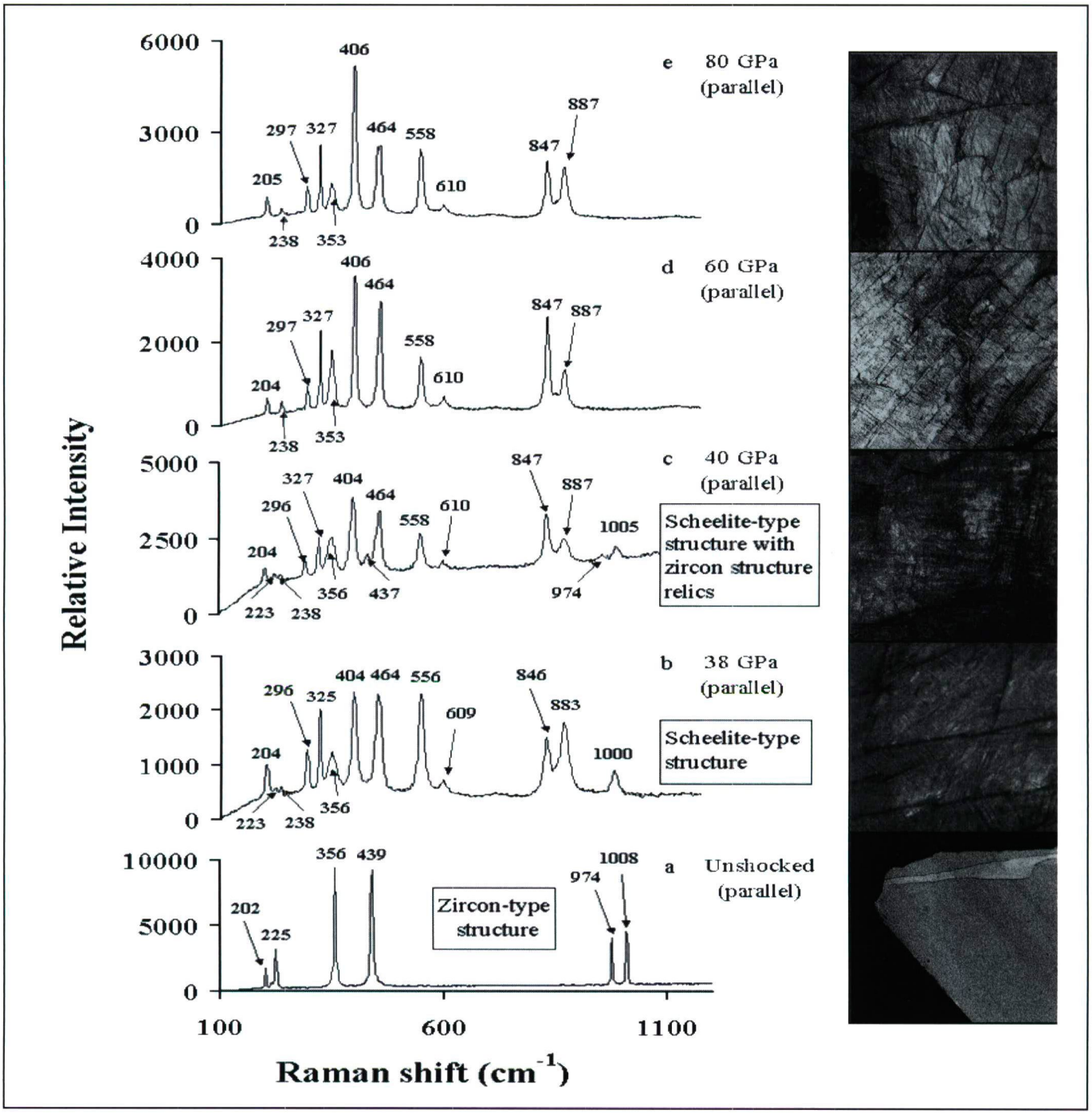

Fig. 3. Raman spectra and CL images of same area of unshocked and experimentally shocked (38, 40, 60, 80 GPa) zircon samples, which were cut parallel to their c-axes. The peaks of the unshocked sample indicate zircon-structure and bands of the shocked samples are characteristic of the high-pressure scheelite-type phase. The 38 and 40 GPa samples, however, exhibit some weak bands that indicate relics of zircon-phase (c). Numbers denote peak positions in [cm^{-1}].

Raman Spectroscopy of naturally shock-deformed zircon samples from the Ries crater

The Raman spectra of the naturally shock-deformed zircon samples from the Ries crater (Stage-II: 35-45 GPa, Stage-III: 45-50 GPa, Stage-IV: >50 GPa) cut parallel and perpendicular to their crystallographic c-axes exhibit differences from each other as it can be seen in Fig. 4. The fluorescence background is considerably higher and Raman bands are wider in all samples than for the experimentally shock-deformed samples, which indicate lower crystallinity with major zoning and defects.

Both Stage-II (35-45 GPa) samples are characterized by five peaks at 224, 356, 439, 974 and 1007 cm-1, indicating zircon-type structure (Williams and Knittle 1993, Kolesov et al. 2001) (Fig. 4A, B). Additionally, a weak peak at 210 cm-1 appears in the Raman spectra of the Stage-II parallel sample (Fig. 4A). The peak intensities of the perpendicular sample are higher than those of the parallel-samples.

The peak at 1007 cm-1 is relatively strong in the perpendicular sample (Fig. 4B).

The Raman spectrum of the Stage-III (45-50 GPa) parallel-sample shows eleven peaks at 202, 224, 327, 356, 404, 439, 465, 558, 845, 974 and 1007 cm-1, which indicates the presence of the scheelite-type phase among predominant zircon-type material (Fig. 4C). In contrast, the Stage-III perpendicular-sample contains only eight peaks at 202, 214, 224, 356, 404, 439, 974 and 1007 cm-1 showing pure zircon-type structure (Fig. 4D). A peak at 1007 cm-1 is relatively strong in the perpendicular-sample (Fig. 4D). In general, the fluorescence background in the parallel-sample is considerably higher than in the perpendicular-sample. In both cases, the peak intensities are similar.

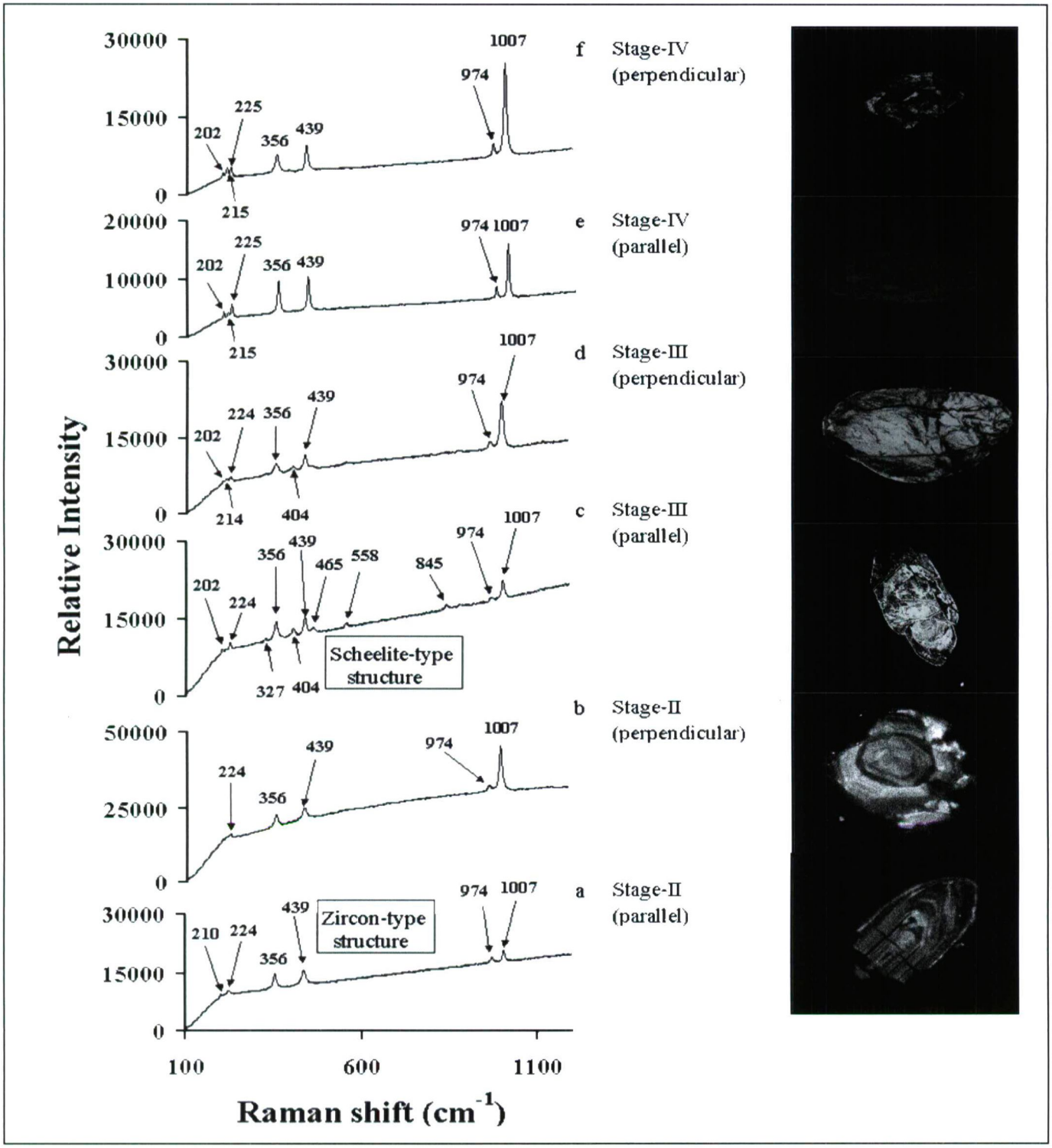

Fig. 4. Raman spectra and CL images of same area of naturally shock deformed zircon specimens from the Ries impact crater (Germany), which were cut parallel and perpendicular to their c-axes including Stage-II, Stage-III and Stage-IV shock stages. The peaks indicate the zircon structure in all shock stages. The bands in the Stage-III parallel-sample indicate also the presence of scheelite-type phase (c). Numbers denote peak positions in [cm^{-1}].

The spectra of the Stage-IV samples (parallel and perpendicular samples) are characterized by seven peaks at 202, 215, 225, 356, 439, 974 and 1007 cm-1, indicating zircon-type phase (Williams and Knittle 1993, Kolesov et al. 2001) (Fig. 4E, F). In both cases, a peak at 1007 cm-1 is relatively strong. The peak intensities of the perpendicular-sample are higher than those of the parallel-sample (Fig. 4F).

Discussion

Raman spectra of natural zircon were described by, e.g., Nasdala et al. (1995) and Kolesov et al. (2001), the spectral signature of the high-pressure scheelite-type phase was reported reported by Williams and Knittle (1993). In general, high-energy modes (at 700-1000 cm-1) might be related to the antisymmetric or symmetric stretching modes of SiO4, whereas low-energy modes (at 100-400 cm-1) might be attributed to the lattice modes. The SiO4 bending modes typically lie in the wave number region of 400-700 cm-1 (Williams and Knittle 1993, Kolesov et al. 2001). The spectra and wave numbers of our Raman modes are in excellent agreement with other studies (Williams and Knittle 1993, Kolesov et al. 2001). Following data presented by Williams and Knittle (1993) and Kolesov et al. (2001), Table 3 and Table 4 give the zircon-and scheelite-type vibrational modes and assignments of the Raman modes observed in this study. The peak positions of scheelite-type modes are very similar to those characteristic of zircon. Even if these features were also observed in the spectra of the high-pressure scheelite-structure phase by Williams and Knittle (1993), there is a high probability that minor amounts of relictic zircon phase material are still present in the 38 and 40 GPa samples. This suggestion is also supported by the TEM investigations of Leroux et al. (1999), who did not observe single-phase scheelite-type material in the 40 GPa (45°-sample), but an epitaxial intergrowth of both phases with a size below the spatial resolution of the micro-Raman spectrometer used in the present study.

Frequency shifts of the 1000 cm-1 band by a few cm-1 might be due to strained zircon caused by shock waves or high-pressure-induced deformation or disorder in zircon. Similar frequency shifts were observed in radiation-damaged zircon (Zhang et al. 2002).

Raman spectra of naturally shock-deformed zircon crystals from the Ries Crater (Stage-II, III and IV) show zircon-type phase. According to Raman spectral measurements and lack of shock-induced planar microdeformations, these samples do not exhibit high-pressure level (the shock pressure that might have been affected the zircon crystals was below 30 GPa). Only the Stage-III (parallel) sample exhibits the presence of traces of scheelite-type vibrational modes, which occur first around 30 GPa (Kusaba et al 1985).

Summary and Conclusions

Raman spectra revealed that the unshocked samples, as well as naturally shock-deformed zircon crystals from the Ries, represent zircon-structure material, whereas the 38 and 40 GPa samples yielded additional peaks with relatively high peak intensities, which are indicative of the presence of the scheelite-type structure of zircon with zircon-structure relics. The 60 and 80 GPa samples display a Raman signature that is characteristic for the existence of only the scheelite-type phase. According to the Raman measurements, the naturally shock-deformed zircons might be related to the low-shock regime (<30 GPa) or recrystallized at the increased post-shock temperature, and do not represent the same shock stages as indicated by whole-rock petrography.

Consequently, the Raman spectroscopy is a potentially useful tool that can be used to characterize the shock stage of zircons from impactites. These results also give new insight into the structural changes that occur in zircons during shock metamorphism, and the pressures associated with these changes.

Table 3. Raman bands and their assignment to vibrational modes of zircon (after Williams and Knittle, 1993; Kolesov et al., 2001).

v_0 (cm^{-1})	Assignment (Raman bands)
1008	v_3: SiO_4 antisymmetric strech
974	v_1: SiO_4 symmetric strech
439	v_2: SiO_4 bend
356	Lattice mode
225	Lattice mode
202	Lattice mode

Table 4. Raman bands and their assignment to vibrational modes of the reidite (scheelite-type structure) (after Williams and Knittle 1993; Kolesov et al. 2001).

v_0 (cm^{-1})	Assignment (Raman bands)
1001	v_3: SiO_4 antisymmetric strech
887	v_3: SiO_4 antisymmetric strech
847	Strain-activated mode
610	v_4: SiO_4 bend
558	v_4: SiO_4 bend
464	v_2: SiO_4 bend
406	Lattice mode
353	Lattice mode
327	Lattice mode
297	Lattice mode
238	Lattice mode
223	Lattice mode
204	Lattice mode

Acknowledgements

As this study was a part of my Ph.D. thesis, I would like to express thank to Profs. Christian Koeberl, Eugen Libowitzky, Uwe Reimold, and Franz Brandstätter supervising my Ph.D. studies at the University of Vienna, Austria. The author is grateful to Dr. Géza Nagy for reviewing this paper.

References

Bohor, B.F., Betterton, W.J., Krogh, T.E. (1993): Impact-shocked zircons: discovery of shock- induced textures reflecting increasing degrees of shock metamorphism. Earth and Planetary Science Letters, **119**, 419–424.

Deloule, E., Chaussidon, M., Glass, B.P., Koeberl, C. (2001): U-Pb isotopic study of relict zircon inclusions recovered from Muong Nong-type tektites. Geochimica et Cosmochimica Acta, **65**, 1833–1838.

DEUTSCH, A. (1998): Examples for terrestrial impact structures. In Marfunin, S.A. (ed.): Mineral Matter in Space, Mantle, Ocean Floor, Biosphere, Environmental Management, and Jewelry, Advanced Mineralogy, Springer-Verlag, Berlin, Heidelberg, 119–129.

DEUTSCH, A., SCHÄRER, U. (1990): Isotope systematics and shock-wave metamorphism: I. U-Pb in zircon, titanite, and monazite, shocked experimentally up to 59 GPa. Geochimica et Cosmochimica Acta, **54**, 3427–3434.

ENGELHARDT, W.v. (1990): Distribution, petrography and shock metamorphism of the ejecta of the Ries crater in Germany - a review. Tectonophysics, **171**, 259–273.

GEOLOGISCHE KARTE DES RIESES, (1999): Bayerisches Geologisches Landesamt, München, 1:50 000

GIBSON, R.L., ARMSTRONG, R.A., REIMOLD, W.U. (1997): The age and thermal evolution of the Vredefort impact structure: A single grain U-Pb zircon study. Geochimica et Cosmochimica Acta, **61**, 1531–1540.

GLASS, B.P., LIU, S. (2001): Discovery of high-pressure $ZrSiO_4$ polymorph in naturally occurring shock-metamorphosed zircons. Geology, **29**, 371–373.

GLASS, B.P., LIU, S., LEAVENS, P.B. (2002): Reidite: An impact-produced high-pressure polymorph of zircon found in marine sediments. American Mineralogist, **87**, 562–565.

GUCSIK, A., KOEBERL, C., BRANDSTÄTTER, F., LIBOWITZKY, E., REIMOLD, W.U. (2004): Cathodoluminescence, electron microscopy, and Raman spectroscopy of experimentally shock metamorphosed zircon crystals and naturally shocked zircon from the Ries impact crater. In Dypvik, H., Burchell, M., Claeys, Ph. (eds.): Cratering in Marine Environments and on Ice, Springer-Verlag, Heidelberg, 281–322.

GUCSIK, A., KOEBERL, C., BRANDSTÄTTER, F., REIMOLD, W.U., LIBOWITZKY, E. (2002): Cathodoluminescence, electron microscopy, and Raman spectroscopy of experimentally shock-metamorphosed zircon. Earth and Planetary Science Letters, **202**, 495–509.

KAMO, S.L., KROUGH, T.E. (1995): Chicxulub crater source for shocked zircon crystals from the Cretaceous-Tertiary boundary layer, Saskatchewan: Evidence from new U-Pb data. Geology, **23**, 281–284.

KAMO, S.L., REIMOLD, W.U., KROGH, T.E., COLLISTON, W.P. (1996): A 2.023 Ga age for the Vredefort impact event and first report of shock metamorphosed zircons in pseudotachylitic breccias and Granophyre. Earth and Planetary Science Letters, **144**, 369–387.

KOLESOV, B.A., GEIGER, C.A., ARMBRUSTER, T. (2001): The dynamic properties of zircon studied by single-crystal X-ray diffaction and Raman spectroscopy. European Journal of Mineralogy, **13**, 939–948.

KROGH, T.E., KAMO, S.L., BOHOR, B.F. (1996): Shock metamorphosed zircons with correlated U-Pb discordance and melt rocks with concordant protolith ages indicate an origin for the Sudbury Structure. In Hart, S., Basu, A. (eds.): American Geophysical Union, Geophysical Monograph **95**, 343–353.

KUSABA, K., SYONO, Y., KIKUCHI, M., FUKUOKA, K. (1985): Shock behaviour of zircon: phase transition to scheelite structure and decomposition. Earth and Planetary Science Letters, 72, 433-439.

LEROUX, H., REIMOLD, W.U., KOEBERL, C., HORNEMANN, U., DOUKHAN, J-C. (1999): Experimental shock deformation in zircon: a transmission electron microscopic study. Earth and Planetary Science Letters, **169**, 291–301.

MCMILLAN, P.F., HOFMEISTER, A.M. (1988): Infrared and Raman spectroscopy. In Hawthorne, F.C. (ed.): Spectroscopic methods in mineralogy and geology, Mineralogical Society of America Reviews, **18**, 99–159.

NASDALA, L., IRMER, G., WOLF, D. (1995): The degree of metamictization in zircon: a Raman spectroscopic study. European Journal of Mineralogy, **7**, 471–478.

OSINSKI, G.R., SPRAY, J.G., GRIEVE, R.A.F. (2003): Impact melting in sedimentary target rocks? Powerpoint Presentation at www.lpi.usra.edu/meetings/impact2003/presentations/osinski8009.ppt

REID, A.F., RINGWOOD, A.E. (1969): Newly observed high pressure transformations in Mn_3O_4, $CaAl_2O_4$, and $ZrSiO_4$. Earth and Planetary Science Letters, **6**, 205–208.

REIMOLD, W.U., LEROUX, H., GIBSON, R.L. (2002): Shocked and thermally metamorphosed zircon from the Vredefort impact structure, South Africa: A transmission electron microscopic study. European Journal of Mineralogy, **14**, 859–868.

ROBERTS, S., BEATTIE, I. (1995): Micro-Raman spectroscopy in the Earth Sciences. In Potts, P.J., Bowles, J.F.W., Reed, S.J.B., Cave, M.R. (eds.): Microprobe techniques in the Earth Sciences. Chapman and Hall, London, 387–408.

SCOTT, H.P., WILLIAMS, Q., KNITTLE, E. (2002): Ultralow compressibility silicate without highly coordinated silicon. Physical Review Letters, **88**, 015506-1-015506-4.

STAUDACHER, T., JESSBERGER, K.E., DOMINIK, B., KRISTEN, T., SCHAEFFER, A.O. (1982): ^{40}Ar-^{39}Ar of rocksand glasses from the Nördlinger Ries crater and the temperature history of impact breccias. Journal of Geophysics, **51**, 1–11.

STÖFFLER, D. (1974): Deformation and transformation of rock-forming minerals by natural and experimental shock processes. Fortschritte der Mineralogie, **49**, 256–298.

WILLIAMS, Q., KNITTLE, E. (1993): High-pressure Raman spectroscopy of $ZrSiO_4$: Observation of the zircon to scheelite transition at 300 K. American Mineralogist, **78**, 245–252.

WITTMANN, A., KENKMANN, T., SCMITT, R.T. STÖFFLER, D. (2006): Shock metamorphosed zircon in terrestrial impact craters. Meteoritics and Planetary Sciences, **40**, 1–16.

Zhang, M., Salje, E.K.H., Ewing, R.C. (2002): Infrared spectra of Si-O overtones, hydrous species, and U ions in metamict zircon: radiation damage and recrystallization. Journal of Physics: Condensed Matter, **14**, 3333–3352.

Received: March 22, 2007; accepted: December 20, 2007